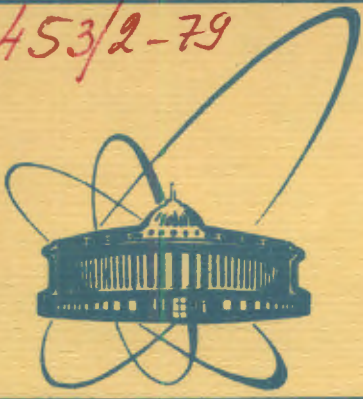


3/1x-79

3453/2-79



объединенный
институт
ядерных
исследований
Дубна

V-35

E2 - 12369

L.Végh

ON THE ELASTIC pd
AND QUASIFREE $A(p,Nd)B$ SCATTERING
AT INTERMEDIATE ENERGIES

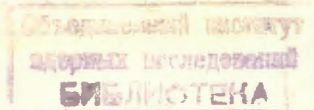
1979

E2 - 12369

L.Végh

ON THE ELASTIC pd
AND QUASIFREE $A(p,Nd)B$ SCATTERING
AT INTERMEDIATE ENERGIES

Submitted to "Journal of Physics, G"



Вег Л.

E2 - 12369

Упругое pd и квазиупругое $A(p, Nd)B$ рассеяние на большие углы при промежуточных энергиях

Приводится теоретическое исследование упругого pd и $p \langle NN \rangle \rightarrow Nd$ рассеяния с помощью модели Крэджи и Вилкина. Сечения $p \langle NN \rangle \rightarrow Nd$ чувствительны только к поведению волновой функции относительного движения $\langle NN \rangle$ на малых расстояниях. Квазиупругий $A(p, Nd)B$ процесс описывается с учётом $p \langle NN \rangle \rightarrow Nd$ амплитуд.

Работа выполнена в Лаборатории ядерных проблем ОИЯИ.

Препринт Объединенного института ядерных исследований. Дубна 1979

Végh L.

E2 - 12369

On the Elastic pd and Quasifree $A(p, Nd)B$ Scattering at Intermediate Energies

Elastic pd and $p \langle NN \rangle \rightarrow Nd$ scattering at backward angles has been studied within the one-pion-exchange model. The $p \langle NN \rangle \rightarrow Nd$ amplitudes depend on the small distance behaviour of the $\langle NN \rangle$ relative wave functions only. The $A(p, Nd)B$ quasifree scattering is described in terms of the $p \langle NN \rangle \rightarrow Nd$ amplitudes.

The investigation has been performed at the Laboratory of Nuclear Problems, JINR.

Preprint of the Joint Institute for Nuclear Research. Dubna 1979

The Cragie-Wilkin model^{/1-3/} assuming the one-pion-exchange (OPE) mechanism describes rather satisfactorily the large angle pd elastic scattering near 660 MeV proton energies. The pd elastic differential cross section due to the OPE diagrams shown in figure 1 is proportional to the $pp \rightarrow d\pi^+$ cross section.

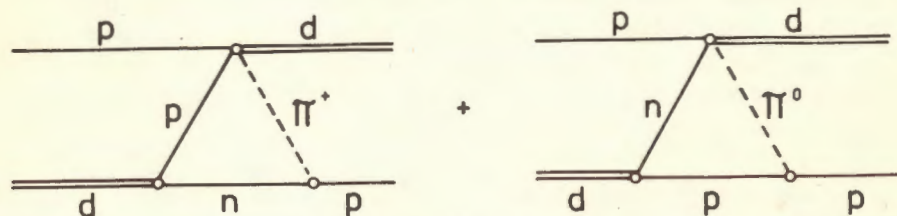


Fig. 1. The OPE triangle diagrams.

The pd elastic analysing power is determined by that of the $pp \rightarrow d\pi^+$ reaction in such a way that they should be equal. The Cragie-Wilkin model affords a good fit to the pd backward elastic scattering over a wide range of energies and angles^{/3/}. Recent measurements have given further confidence to the model. Confirming the results^{/4,5/} the data^{/6/} on nd elastic scattering at extremely backward angles over the incident energy range of 200-800 MeV show a striking shoulder in the excitation function for neutron energies of 300-600 MeV. This shoulder can be explained in the OPE model by the resonance character of the $pp \rightarrow d\pi^+$ process, and the nd excitation function can be fitted assuming a one-nucleon-exchange

like background^{/2/}. A strong similarity has been found between the analysing power data for pd elastic scattering and those for pp → dπ⁺ reaction in the region of 590-720 MeV^{/7,8/}. These experiments suggest that the main contribution to the pd elastic cross sections at backward angles in the 550-750 MeV proton energy region is given by the OPE mechanism, and the background terms are not too important. The analysing power measurements^{/7,9/} show that the OPE diagram no longer dominates at energies lower than 500 MeV and higher than 1 GeV.

The different versions of the Cragie-Wilkin model contain information on deuteron structure in different ways. Kolybasov and Smorodinskaya^{/2/} expressed the dpn vertex of the OPE diagrams in terms of the ψ_d(r̄) deuteron wave function, and the cross section depends rather sensitively on the small distance behaviour of ψ_d(r̄). The pd → pd differential cross section can be expressed as follows (ħ = c = 1):

$$\frac{d\sigma^{pd \rightarrow pd}}{d\Omega_\phi} = \frac{3}{2} \frac{G^2}{4\pi} F^2(k^2) \frac{E_2+m}{E_2^2} (f_{01}^2 + f_{21}^2) \frac{s_{pp} |p|}{s_{pd} |d|} \frac{3}{2} \frac{d\sigma^{pp \rightarrow d\pi^+}}{d\Omega_\theta} \equiv (f_{01}^2 + f_{21}^2) A^2(s_{pd}, u_{pd}) \quad (1)$$

$$f_{\ell\ell_1} = \int_0^\infty e^{-\gamma r} \psi_{d\ell}(r) (1 + \gamma r) j_{\ell_1}(p_3 r) dr,$$

$G^2/4\pi = 14.7$, $F(k^2)$ is the Ferrari-Selleri factor^{/10/}. The invariant k^2 , s_{pp} , s_{pd} , u_{pd} , $|p|$, $|d|$ symbols and the relation between $\cos\phi$ and $\cos\theta$ with the $\cos\theta$ fixed prescription are defined in^{/3/}. m is the nucleon mass, $E_2 = T_2 + m$ is the energy of outgoing proton, the T_2 kinetic energy can be expressed by k^2 as $T_2 = k^2/M_d$, M_d is the deuteron mass. $A^2(s_{pd}, u_{pd})$ is defined by the equation. $\gamma^2 = T_2^2 / (1 + T_2/m)^2 + \mu^2 / (1 + T_2/m)$, μ is the pion mass. This γ^2 differs from the γ^2 used by Kolybasov and Smorodinskaya, where its first term had a wrong minus sign.

$p_3 = |\vec{p}_2 / (1 + T_2/m) - \vec{d}_0 / 2|$, where \vec{d}_0 is the initial deuteron and \vec{p}_2 the outgoing proton momentum. This p_3 is not relativistic invariant and we use the invariant $p_3 = 1 / (1 + T_2/m)(T_2^2 + k^2)^{1/2}$ prescription.

The cross sections with Hulthen and realistic Reid soft-core, Reid hard-core^{/11/} and Bressel-Kerman-Wentzel^{/12/} deuteron wave functions as $\psi_d(\vec{r})$ are presented in figure 2. The experimental points for 582 MeV proton energies are taken from^{/13/} and the pp → dπ⁺ experimental cross sections used in the

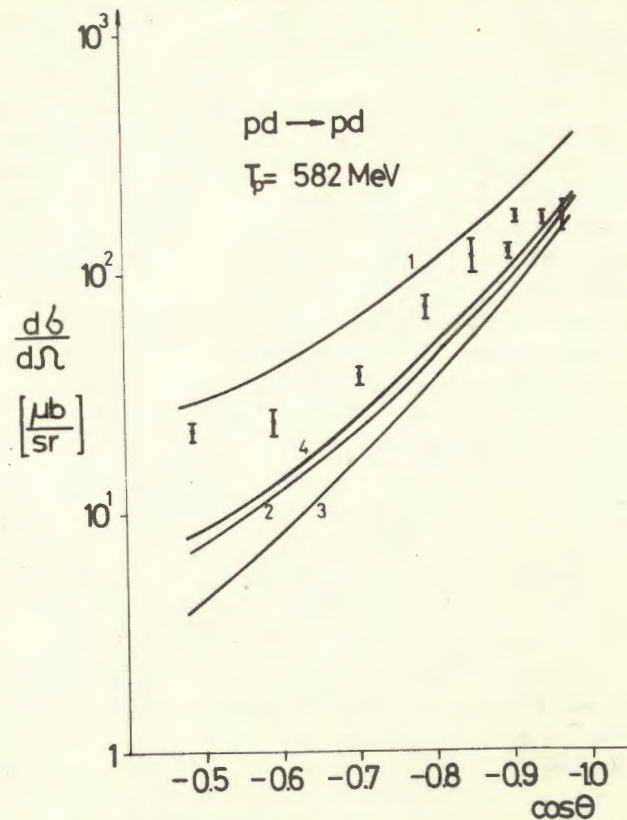


Fig.2. The pd elastic cross section due to the OPE diagram with Hulthen (1), Reid soft-core (2), Reid hard-core (3) and Bressel-Kerman-Wentzel (4) deuteron wave functions. The experimental points are taken from^{/13/}.

calculation are from^{14/}. The cross sections calculated with realistic wave functions agree well with experiment. At backward angles, the 10-20 percent deviations in their values are due to the differences in the wave functions within 1fm. The $\ell=2$ components of the wave functions give a contribution about 10 percent to the cross sections. The basic approximation in derivation of cross section formulae (1) is the peaking approximation, that is, the $pp \rightarrow d\pi^+$ amplitudes are replaced by their value at zero relative pn momentum in the deuteron. The effect of this uncertainty may be estimated to be 20 percent in cross section in this energy region. The effect of background is hard to estimate, its neglect at backward angles may give another 10 percent contribution to the cross section^{12/}. As there are other smaller approximations in the model, too, we are not able to select among the accepted deuteron wave functions.

The $f_{\ell\ell_1}$ integral strongly depends on the small distance behaviour of the deuteron wave functions. As, for example, for $T_2=60$ MeV $\gamma=0.74$ fm⁻¹ and $T_2=100$ MeV $\gamma=0.80$ fm⁻¹, respectively, the cross section in this region is determined by the $\psi_{d\ell}(\vec{r})$ wave function values for $r \leq 1.5$ fm. For example, at small distances the Hulthen wave function has larger values than the realistic wave functions and these differences give about a factor of two in the cross sections in figure 2. The cross section has been evaluated also with Hulthen wave functions cut off at different r_c distances (for $r \leq r_c$ $\psi(\vec{r})=0$, for $r > r_c$ $\psi(\vec{r})$ is equal to the normalized Hulthen function). Figure 3 shows the drastic decrease of the calculated pd cross section with increase of r_c from 0 to 1.5 fm. A Hulthen wave function with a hard core radius of 0.5-0.6 fm may fit $pd \rightarrow pd$ experimental data.

The dependence of elastic pd amplitudes on the short range part of the initial deuteron wave function makes it possible to study the short range part of the $\langle np \rangle$ and $\langle nn \rangle$ two nucleon wave functions inside the nucleus. Considering the isospin invarian-

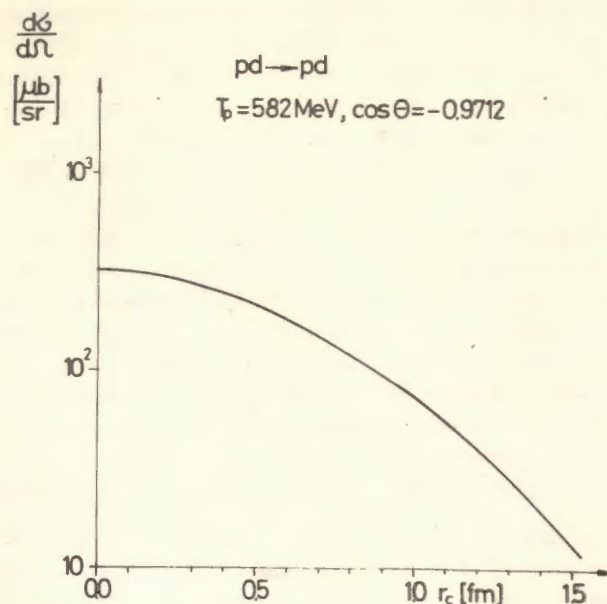


Fig.3. The pd elastic cross section evaluated with the Hulthen wave function cut off at different r_c .

ce, formula (1) can be extended for the calculation of the $p \langle NN \rangle \rightarrow Nd$ cross sections, where the $\langle NN \rangle$ pair has isospin t with projection ν . For example, the sum of the two diagrams in figure 1 is coherent only for $\langle np \rangle$ pairs with $t=0$. Assuming identical space wave functions this gives a factor of 9 for the $\sigma(pd \rightarrow pd)/\sigma(pd \rightarrow pd)$ ratio, where d is the singlet deuteron. The extension of the formalism for $\langle NN \rangle$ pair with arbitrary j angular momentum and s spin is straightforward, too. The general $p \langle NN \rangle \rightarrow Nd$ cross section formula valid for the $\langle NN \rangle$ nucleon pair with $t\nu j_s$ quantum numbers is the following

$$\frac{d\sigma_{p \langle NN \rangle \rightarrow Nd}}{d\Omega_\Phi} = n_{t\nu} \left[\sum_{\ell} U(1/2 \ 1/2 j \ell; s \ell - 1/2)^2 f_{\ell\ell-1}^2 + \right. \\ \left. + U(1/2 \ 1/2 j \ell; s \ell + 1/2)^2 f_{\ell\ell+1}^2 \right] A^2(s_{pd}, u_{pd}), \quad (2)$$

where ℓ are the orbital momenta corresponding to the parity of the given state, $U(j_1 j_2 j_3 ; j_{12} j_{23})$ is the Jahn coefficient^{15/} $n_{00}=1, n_{10}=1/9, n_{1-1}=2/9$. If the bombarding particle is a neutron we are able to investigate the $\langle pp \rangle$ and $\langle pn \rangle$ pairs. Formulae (2) is valid for the calculation of the $n \langle NN \rangle \rightarrow Nd$ cross sections if $n_{00}=1, n_{10}=1/9, n_{11}=2/9$.

The $\langle NN \rangle$ relative wave functions inside the nucleus can be extracted from different nuclear models. Using, for example, the shell model it is convenient to apply as basis the harmonic oscillator wave functions (HOWF) while using the Talmi transformation^{16/} the product of two single particle HOWF can be expanded by the products of HOWF depending on the relative and c.m. coordinates.

The higher the ℓ , the smaller the $f_{\ell\ell+1}^2$ integrals, as with increasing ℓ the inert region of the integral becomes empty due to the small distance behaviour of $\psi_\ell(r)$ and the $j_{\ell+1}^{-1}(p_3 r)$ Bessel functions. We have calculated the $f_{\ell\ell+1}^2$ factors using HOWF with $n=0$ radial quantum number as functions of the harmonic oscillator length parameter r_0 . The results for r_0 values corresponding to a wide region of nuclear masses are shown in figure 4. It can be seen that the $f_{\ell\ell+1}^2$ values are essentially larger for $\ell=0$ than those for $\ell \neq 0$. The picture remains the same for different n values, too. Therefore, the $\ell > 0$ components of the same weight as that for $\ell=0$ can be neglected. However, the ℓ dependence of $f_{\ell\ell+1}^2$ shown in figure 4 does not contradict the fact that the deuteron wave functions give a relatively large $\ell=2$ contribution. Namely for the free np interaction the strongly attractive tensor force with $s=1, \ell$ even compensates the repulsing effect of the centrifugal potential. In the average potentials which determine the single particle wave functions the tensor forces are concealed.

In order to study the $\langle NN \rangle$ pairs inside the nucleus the investigation of $A(p, Nd)B$ quasifree scattering may be a useful tool. A description similar to that

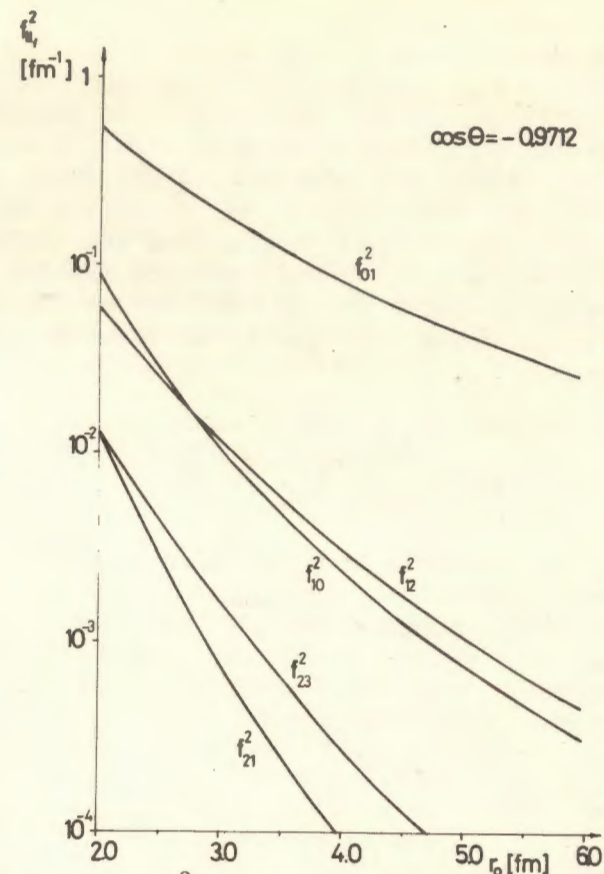


Fig.4. The $f_{\ell\ell+1}^2$ factors calculated with harmonic oscillator wave functions dependence on the r_0 harmonic oscillator length parameter.

applied for $A(p, p'd)B$ quasifree knockout reaction^{17/} seems to be applied for this case, too. The main difference between the two description is that we do not project out the deuteron states from the nuclear wave function and we do not take the free $pd \rightarrow pd$ cross section from other sources. We may describe the $A(p, p'd)B$ cross section in the given energy and angle range directly in terms of the calculated $\langle pn \rangle \rightarrow pd$ amplitudes.

For the description of the $A(p, Nd)B$ reaction we closely follow the treatment of Chant and Roos ^{/18/}. They give a formalism for distorted-wave impulse-approximation calculations of quasifree cluster knockout reactions. Not identifying the deuteron with the initial $\langle NN \rangle$ cluster our formalism becomes a little more complicated. Neglecting the amplitudes with $\ell > 0$ relative $\langle NN \rangle$ orbital momenta the $A(p, Nd)B$ cross section contains the $pp \rightarrow d\pi^+$ cross section in separate form. Using the symbols of formula (1) and (2) we obtain:

$$\frac{d\sigma_{pA \rightarrow NdB}}{d\Omega_{\Phi}} = A^2 (s_{pd} u_{pd}) \frac{k_N k_d}{k_p E_{NN}} H \sum_{\alpha \alpha'} n_{\ell} f_{01}^{a \ell \nu} f_{01}^{a' \ell \nu} S_{BA}^{a \ell \nu} \sum_{\Lambda} T_{BA}^{a \ell \Lambda} T_{BA}^{a' \ell \Lambda*} \quad (3)$$

The k_N, k_d, k_p momenta and the E_{NN} energy are taken in laboratory system. L with projection Λ is the relative angular momentum of $\langle NN \rangle$ and the B residual nucleus and all the other quantum numbers necessary to specify the given state are denoted by α . The $T_{BA}^{a \ell \Lambda}$ distorted momentum distribution function and the additional H phase space factor are defined in ^{/18/}. $S_{BA}^{a \ell \nu}$ can be given by the $S_{\alpha Lst}$ spectroscopic factor ^{/18/}

$$S_{BA}^{a \ell \nu} = C^2 \sum_s S_{\alpha Lst}^{1/2} S_{\alpha' Lst}^{1/2},$$

but $S_{\alpha Lst}$ now relates to the $\langle NN \rangle$ pair with s spin, t isospin and with $\ell=0$ relative orbital momentum. C is the $(T_B N_B t \nu T_A N_A)$ Clebsch-Gordan coefficients, T_A (projection N_A) and T_B (projection N_B) are the isospin quantum numbers for the target and residual nuclei, respectively.

For the nuclei containing two or three extra nucleons outside the closed shells the calculation of cross section (3) is relatively simple. Studying large-angle $N-d$ coincidence experiments for very light nuclei ^{/19/} or those with good energy resolution, the reactions on the extra nucleus can be separated.

The determination of the spectroscopic factors of $\langle NN \rangle$ pairs with $\ell=0$ is relatively simple for extra nucleons. The distortion effects are relatively small at higher energies and $T_{BA}^{a \ell \Lambda}$ can be calculated in eikonal approximation. Using different $\langle NN \rangle$ relative wave functions, information for $\psi(r)$ in the region of small r ($r \leq 1.5$ fm) can be obtained by fitting the (3) cross section formula to the experimental data. Such investigations may give new information on NN interactions inside the nucleus.

I would like to thank J. Erö, B.Z. Kopeliovich and L.I. Lapidus for helpful discussions.

REFERENCES

1. Craigie N.C., Wilkin C. Nucl.Phys., 1969, B14, p. 477.
2. Kolybasov V.M., Smorodinskaya N.Ya. Phys.Lett., 1971, 37B, p. 272; Yad.fiz., 1973, 17, p. 1211.
3. Barry G.W. Ann.Phys., (N.Y.), 1972, 73, p. 482.
4. Alder J.C. et al. Phys.Rev., 1972, C6, p. 2010.
5. Komarov V.I. et al. Yad.fiz., 1972, 16, p. 234.
6. Bonner B.E. et al. Phys.Rev.Lett., 1977, 39, p. 1253.
7. Biegert E. et al. Phys.Rev.Lett., 1978, 41, p. 1098.
8. Murtazaev Kh., Nadezhdin V.S., Satarov V.I. Zh. eksp.teor.fiz., 1978, 27, p. 336.
9. Anderson A. et al. Phys.Rev.Lett., 1978, 40, p. 1553.
10. Ferrari E., Selleri F. Phys.Rev.Lett., 1961, 7, p. 387.
11. Reid R.V. Jr. Ann.Phys., (N.Y.), 1968, 50, p. 411.
12. Bressel C.N., Kerman A.R., Rouben B. Nucl.Phys., 1968, A124, p. 624.
13. Vincent J.S. et al. Phys.Rev.Lett., 1970, 24, p. 236.
14. Richard-Serre C. et al. Nucl.Phys., 1970, B20, p. 413.
15. Jahn H.A. Proc.Roy.Soc., 1951, A205, p. 192.

16. Talmi I. *Helv.Phys.*, 1952, 25, p. 185.
17. Sakamoto Y. *Phys.Rev.*, 1964, 134, B1211.
18. Chant N.S., Roos P.G. *Phys.Rev.*, 1977, C15, p. 15.

Received by Publishing Department
on April 6 1979.